

Ectopic Expression of Human MutS Homologue 2 on Renal Carcinoma Cells Is Induced by Oxidative Stress with Interleukin-18 Promotion via p38 Mitogen-activated Protein Kinase (MAPK) and c-Jun N-terminal Kinase (JNK) Signaling Pathways^{*[5]}

Received for publication, February 10, 2012, and in revised form, April 6, 2012. Published, JBC Papers in Press, April 9, 2012, DOI 10.1074/jbc.M112.349936

Chen Mo^{†§}, Yumei Dai[†], Ning Kang^{†§}, Lianxian Cui^{†§}, and Wei He^{†§1}

From the [†]Department of Immunology, Institute of Basic Medical Sciences, Chinese Academy of Medical Sciences and School of Peking Union Medical College, Beijing 100005, China and the [§]National Key Laboratory of Medical Molecular Biology, Beijing 100005, China

Background: Ectopically expressed MutS homologue 2 (hMSH2) is a ligand of $\gamma\delta$ T cells.

Results: Oxidative stress induces ectopic expression of hMSH2 on renal carcinoma cells with IL-18 promotion via p38 MAPK and JNK pathways, promoting $\gamma\delta$ T cell-mediated lysis of renal tumor cells.

Conclusion: Ectopically expressed hMSH2 is induced under stressful conditions.

Significance: We reveal a mechanism of ectopic hMSH2 expression and its contribution to $\gamma\delta$ T cell-mediated immunosurveillance in stress.

Human MutS homologue 2 (hMSH2), a crucial element of the highly conserved DNA mismatch repair system, maintains genetic stability in the nucleus of normal cells. Our previous studies indicate that hMSH2 is ectopically expressed on the surface of epithelial tumor cells and recognized by both T cell receptor $\gamma\delta$ (TCR $\gamma\delta$) and natural killer group 2 member D (NKG2D) on V δ 2 T cells. Ectopically expressed hMSH2 could trigger a $\gamma\delta$ T cell-mediated cytotoxicity. In this study, we showed that oxidative stress induced ectopic expression of hMSH2 on human renal carcinoma cells. Under oxidative stress, both p38 mitogen-activated protein kinase (MAPK) and c-Jun N-terminal kinase (JNK) pathways have been confirmed to mediate the ectopic expression of hMSH2 through the apoptosis-signaling kinase 1 (ASK1) upstream and activating transcription factor 3 (ATF3) downstream of both pathways. Moreover, renal carcinoma cell-derived interleukin (IL)-18 in oxidative stress was a prominent stimulator for ectopically induced expression of hMSH2, which was promoted by interferon (IFN)- γ as well. Finally, oxidative stress or pretreatment with IL-18 and IFN- γ enhanced $\gamma\delta$ T cell-mediated cytotoxicity of renal carcinoma cells. Our results not only establish a mechanism of ectopic hMSH2 expression in tumor cells but also find a biological linkage between ectopic expression of hMSH2 and activation of $\gamma\delta$ T cells in stressful conditions. Because $\gamma\delta$ T cells play an important role in the early stage of innate anti-tumor response, $\gamma\delta$ T cell activation triggered by ectopically expressed hMSH2 may be an important event in immunosurveillance for carcinogenesis.

The DNA MMR² system plays a central role in maintaining genetic stability by inhibiting base-base mismatches and insertion/deletion mispairs generated during DNA replication and recombination (1, 2). Homologs of bacterial MMR proteins MutS and MutL in eukaryotes have received much attention because of many discoveries showing a linkage between human cancer and MMR defects (3). The critical role of the MMR system in carcinogenesis is exemplified by the fact that hereditary nonpolyposis colorectal cancer occurs primarily due to heterozygous germ line mutations in the MMR genes: *hMLH1* (MutL homolog 1), *hMSH2*, *hMSH6* (MutS homologue 6), and *hPMS2* (MutL homologue) (4). The *hMLH1* promoter hypermethylation has been observed in ovarian, endometrial, gastric, and colorectal carcinoma (5). The *hMSH2* mutations have a higher incidence of extracolonic tumors (6). The defects of both MMR genes are involved in renal carcinogenesis and correlate with the occurrence of microsatellite instability (7).

Under physiological conditions, hMSH2 is mainly synthesized in cytoplasm and transported into the nucleus together with MutS homologue 3 (hMSH3) or hMSH6 to maintain the DNA replication fidelity (8, 9). Increased expression of hMSH2 RNA and/or protein has been reported in various malignancies (10–14). However, the underlying mechanism that causes increased levels of hMSH2 in malignancies is yet unknown. Previously, we found an unusual expression of hMSH2 on the surface of human ovarian carcinoma cells, and ectopically expressed hMSH2 promoted the lysis of ovarian carcinoma cells by $\gamma\delta$ T cells (15). We also identified that ectopically expressed hMSH2 could be recognized by $\gamma\delta$ T cells through the interaction with both TCR $\gamma\delta$ (T cell receptor $\gamma\delta$) and

* This work was supported by National Natural Science Foundation of China Grant 30930083.

[5] This article contains supplemental Figs. 1 and 2.

¹ To whom correspondence should be addressed: Dept. of Immunology, Institute of Basic Medical Sciences, Chinese Academy of Medical Sciences and School of Peking Union Medical College, National Key Laboratory of Medical Molecular Biology, 5 Dong Dan San Tiao, Beijing 100005, China. Tel./Fax: 86-10-68792233; E-mail: hewei@moh.gov.cn.

² The abbreviations used are: MMR, mismatch repair; DAMP, damage-associated molecular pattern; ROS, reactive oxygen species; RCC, renal cell carcinoma; GO, glucose oxidase; NAC, N-Acetyl-L-cysteine; Ab, antibody.

NKG2D (natural killer group 2 member D) (77). However, the mechanism of ectopic expression of hMSH2 in tumor cells is unclear, and ectopic hMSH2 expression may be important for the recognition of potential damage-associated molecular patterns (DAMPs) by human $\gamma\delta$ T cells (16–18).

Oxidative stress, defined as the imbalance between the generation of reactive oxygen species (ROS) and scavenging by antioxidant defenses of the cell, is involved in carcinogenesis because it induces DNA damage and causes oxidative modification (19). The tumorigenicity of oxidative stress has been observed among various carcinomas, especially in RCC cells, which possess low antioxidant capacities as a consequence of the absence of peroxisomes and the changed redox status (20, 21). The defective antioxidant capacity also produces a prooxidant environment in RCC cells and promotes the process of renal tumor genesis (20, 22).

Because hMSH2 or hMSH6 participates in removing complex DNA lesions produced in oxidative stress (23), we hypothesize that oxidative stress may be responsible for ectopic expression of hMSH2 on tumor cells. In the present study, we established a glucose oxidase (GO)-mediated oxidative stress model in RCC cells through oxidizing β -D-glucose and generating hydrogen peroxide (H_2O_2) continuously at a relatively low level (24). We found that hMSH2 was constitutively expressed at a low level on the surface of RCC cells. However, ectopic expression of hMSH2 was increased in GO-mediated oxidative stress through p38 MAPK and JNK pathways in RCC cells. The regulating role of p38 MAPK and JNK pathways was mediated by a node kinase, ASK1, upstream and the stress-sensitive activating transcription factor 3 (ATF3) downstream of both pathways. Moreover, proinflammatory cytokine IL-18 produced by RCC cells was a crucial stimulator inducing ectopic expression of hMSH2 in oxidative stress. Meanwhile, exogenous IFN- γ further promoted ectopic expression of hMSH2 on the surface of RCC cells, and $\gamma\delta$ T cells produced a high level of IFN- γ during oxidative stress. We also showed that oxidative stress or IL-18 enhanced $\gamma\delta$ T cell-mediated lysis of RCC cells. Taken together, our finding provides a better understanding of oxidative stress-induced ectopic expression of hMSH2 on the surface of RCC cells. As a result, ectopically expressed hMSH2 may act as a candidate molecule of DAMPs recognized by $\gamma\delta$ T cells, which indicates that $\gamma\delta$ T cells may perform immunosurveillance of hMSH2-bearing tumor cells in an oxidative stress environment.

EXPERIMENTAL PROCEDURES

Chemicals—The glucose oxidase (G7141) catalyzes the oxidation of β -D-glucose into D-glucono- β -lactone and H_2O_2 , with molecular oxygen as an electron acceptor. *N*-Acetyl-L-cysteine (NAC) (A7250), a ROS scavenger, was selected to block the H_2O_2 effect. Calyculin A from *Discodermia calyx* (C5552) was used as an inhibitor of protein phosphatases types 1 and 2A. The reagents above were purchased from Sigma-Aldrich. Pharmacological inhibitors of p38 MAPK (SB203580) and JNK (420119) were purchased from Merck, and the inhibitors of the MAPK/ERK kinase (MEK) and ERK pathway (U0126) were purchased from Selleck. The 1-methylpropyl 2-imidazolyl disulfide (PX-12) was purchased from TOCRIS.

Cell Culture and Treatment—Human renal carcinoma cell line G401, melanoma cell line A375, lymphoma cell line Jurkat, and leukemia cell line K562 were maintained in RPMI 1640 medium (Invitrogen) supplemented with 10% FCS (Invitrogen). Human renal carcinoma cell line A498 was maintained in minimum Eagle's medium supplemented with 10% FBS (Hyclone). Human renal proximal tubule epithelial cell line HK-2 was maintained in DMEM/F-12 medium supplemented with 10% FCS (Invitrogen). All cell lines were obtained from the Cell Center, Institute of Basic Medical Sciences, Chinese Academy of Medical Sciences (Beijing, China). For constructing the oxidative stress model, the cells were activated by different concentrations of glucose oxidase (G7141; Sigma) in medium at 37 °C, 5% CO_2 for prospective times (24).

$\gamma\delta$ T Cell Expansion in Vitro—Peripheral blood mononuclear cells from healthy donors were isolated by Ficoll-Hypaque (TBD, Tianjin, China) centrifugation. $\gamma\delta$ T cells were expanded as described previously (25). Briefly, 24-well plates were coated with 500 μ l of purified anti-TCR $\gamma\delta$ antibody (Ab) (IMMU510; 1 μ g/ml; Immunotech, Beckman Coulter) at 37 °C, 5% CO_2 for 2 h. Peripheral blood mononuclear cells were transferred to the plate and cultured in RPMI 1640 medium supplemented with 10% FCS and recombinant human IL-2 (200 IU/ml; Beijing Read United Cross Pharmaceutical Co., Ltd., Beijing, China). After 2 weeks of culture, the purity of $\gamma\delta$ T cells was more than 90% as assessed by flow cytometry analysis and ready for further use.

Cytotoxicity Assay—Cell cytotoxicity was determined by the CytoTox 96[®] non-radioactive cytotoxicity assay kit (Promega). G401 cells were preincubated with the indicated amounts of GO, IL-18, or IL-18 plus IFN- γ . $\gamma\delta$ T cells of appropriate number were incubated with G401 cells (1×10^5 /ml) in triplicates for 4 h at 37 °C. The release of lactate dehydrogenase and percentage of cytotoxicity were determined by the absorbance of supernatants at 490 nm.

RNA Interference—A pool of three specific 19–25-nt small interfering RNA (siRNA) designed to knock down *IL-18R α* expression (sc-45285), mock control siRNA-A (sc-37007), and the transfection reagent (sc-29528) was purchased from Santa Cruz Biotechnology, Inc. Three pairs of StealthTM RNAi-specific *ATF3* siRNA were purchased from Invitrogen: senseI, 5'-GAGGCGACGAGAAAGAAAUAAGAUU-3'; antisenseI, 5'-AAUCUUUUUCUUUCUCGUCGCCUC-3'; senseII, 5'-GCAGCUGCAAAGUGCCGAAACAAGA-3'; antisenseII, 5'-UCUUGUUUCGGCACUUUGCAGCUGC-3'; senseIII, 5'-GGGAGGACUCCAGAAGAUGAGAGAA-3'; antisenseIII, 5'-UUCUCUCAUCUUCUGGAGUCCUC-3'. StealthTM RNAi universal negative control Med GC duplex (Invitrogen) were used as mock control. All of these siRNA duplexes were transfected using LipofectamineTM RNAiMAX according to manufacturer's instructions (Invitrogen). The delivery of siRNAs was measured by transfection with BLOCK-iTTM Alexa Fluor[®] Red Fluorescent Oligo (Invitrogen) and analyzed at 12 h after transfection. Efficiency of target genes knockdown was evaluated by quantitative real-time RT-PCR and Western blot.

Real-time RT-PCR—Total RNA was isolated from G401 cells with the TRIzol reagent (Invitrogen). The cDNA was syn-

Oxidative Stress Induces Ectopic Expression of hMSH2

thesized using oligo(dT) as primers and the Moloney murine leukemia virus reverse transcriptase (Promega) in the reverse transcription reaction. The specific primers used were as follows: for *IL-18R α* , 5'-ACCCTTTGGGTGCTTATATCTGTAA-3' (forward) and 5'-GTTCCCCTCAACCACAGTATG-3' (reverse); for *hMSH2*, 5'-TTCATGGCTGAAATGTGGA-3' (forward) and 5'-ATGCTAACCCAAATCCATCG-3' (reverse); for *ATF3*, 5'-GCCATTGGAGAGCTGTCTT-3' (forward) and 5'-AAGGGCCTGCTGAATCACT-3' (reverse); for β -actin, 5'-AGAAAATCTGGCACCACACC-3' (forward) and 5'-TAGCACAGCCTGGATAGCAA-3' (reverse). The quantitative PCR was performed in an Applied Biosystems 7500 Fast Real-time PCR System to quantify the levels of *IL-18R α* , *hMSH2*, and *ATF3* mRNA. The amplification reaction was performed using SYBR Green PCR Master Mix (Applied Biosystems, Warrington, UK). Cycling conditions were at 95 °C for 10 min, 40 cycles at 95 °C for 15 s, and at 58 °C for 45 s. Data were analyzed using Sequence Detection Software (version 1.2; Applied Biosystems).

Enzyme-linked Immunosorbent Assay (ELISA) Analyses—The IL-18 in the oxidative stress-stimulated RCC, A375, Jurkat, or K562 cell culture supernatants and IFN- γ or tumor necrosis factor- α (TNF- α) in the oxidative stress-stimulated $\gamma\delta$ T cells culture supernatants were determined by ELISA kits (R&D Systems). The assay procedure was performed according to the manufacturer's instructions.

Western Blotting—Cell lysates were prepared by CytoBusterTM protein extraction reagent (71009, Novagen) for total protein and by the NucBuster protein extraction kit (71183-3, Novagen) for nucleoprotein. Halt Protease and Phosphatase Inhibitor Single-Use Mixture, EDTA-Free (Thermo) were used to prevent enzymatic protein degradation during extraction procedures. The protein concentration was quantified by the Pierce BCA protein assay kit (23227, Thermo). An equal amount of proteins per sample was separated by 12% SDS-PAGE and blotted onto nitrocellulose membranes. The blots were treated with PBS containing 5% skim milk or bovine serum albumin overnight and probed with primary Ab at room temperature for 2 h, followed by the relevant secondary Ab for 1 h. Protein bands were visualized using SuperSignal West Pico Chemiluminescent Substrate (NCI5079, Thermo). Monoclonal antibody (mAb) against phospho-JNK/phospho-p38/phospho-c-Jun (Cell Signaling Technology), anti-human IL-18R α (R&D Systems), ATF3 (Abgent), hMSH2 (ProteinTech Group, Inc.), or β -actin (Signalchem) and polyclonal antibody to histone H3 (Abcam) were used as primary Abs.

Flow Cytometry—Cells were washed with PBS containing 1% BSA, stained with relevant Abs, and incubated at 4 °C for 30 min. Then the cells were washed and resuspended in 300 μ l of PBS containing 1% formaldehyde. FITC-conjugated anti-human IL-18R α Ab (catalog no. 313810), APC-conjugated anti-human MICA/B Ab (catalog no. 320908), and the respective isotype control mAbs were purchased from Biolegend (San Diego, CA). Ab FITC-conjugated anti-TCR $\gamma\delta$ (IMMU510) was purchased from Immunotech. When purified anti-MSH2 Ab (H-300) (sc-22771) and the isotype control polyclonal Abs (Santa Cruz Biotechnology, Inc.) were used as primary Abs, FITC-conjugated goat anti-rabbit secondary Ab (Zhongshan,

China) was then added and incubated for 30 min at 4 °C. For intracellular staining, the cells incubated with 20 ng/ml phorbol 12-myristate-13-acetate (Sigma), 0.5 μ g/ml ionomycin (Sigma), and 3 μ g/ml brefeldin A (eBioscience, San Diego, CA) acted as the positive control. After 4 h, the cells were collected and stained for surface markers. Then the cells were fixed, permeabilized, and incubated with intracellular Abs. All samples were analyzed on an Accuri C6 flow cytometer (BD Biosciences). Data analysis was carried out with FlowJo Software (version 7.6.4, Tree Star, Inc.).

Statistical Analysis—Data were expressed as the mean \pm S.D. and were representative of at least three independent experiments. One-way analysis of variance (SPSS version 16.0 software) was used to determine significant differences between groups. Differences were considered statistically significant at a *p* value of less than 0.05.

RESULTS

Oxidative Stress Induces Ectopic Expression of hMSH2 on Surface of RCC Cells—To determine the ectopic expression of hMSH2 in stress, renal carcinoma cell lines G401 and A498 and a renal proximal tubular cell line, HK-2, were chosen because these cell lines from kidney exhibited a constitutive ectopic expression of hMSH2 on surfaces in normal cultures (Fig. 1A). In response to oxidative stress, ectopically expressed hMSH2 was induced on G401 cells treated by different concentrations of GO for 24 or 36 h, respectively (Fig. 1B). HK-2 and A498 cells showed similar results (data not shown). GO stimulation at 100 ng/ml for 36 h induced the strongest expression in all three cell lines (Fig. 1, B and C). A down-regulation of GO-induced hMSH2 ectopic expression was observed on G401, A498, and HK-2 cells by the addition of NAC, a ROS scavenger that strongly blocks the H₂O₂ effect (Fig. 1, B and C). Because G401 cells exhibited the most obvious changes of ectopically expressed hMSH2 mediated by GO or NAC, we subsequently chose G401 cells as the cell model to investigate the mechanisms underlying ectopic expression of hMSH2 in oxidative stress. An increase of *hMSH2* mRNA was observed as early as 1 h and lasted to 48 h by exposing G401 cells to 100 ng/ml GO-mediated stress (Fig. 1D). Accordingly, the total protein level of hMSH2 was up-regulated in G401 cells stimulated by GO (Fig. 1E). These results demonstrate that ectopic expression of hMSH2 on the surface of RCC cells is induced in response to oxidative stress.

We also found that oxidative stress-induced ectopic expression of hMSH2 showed a similar change pattern to surface expression of MICA/B, classical stress-sensitive ligands of NKG2D in oxidative stress (Fig. 1, F–I), and both of them could be reduced markedly by NAC processing (Fig. 1, F–I). Because expression of MICA/B is restricted or absent in normal tissues and up-regulated in stress and diseases (26, 27), it further confirms the stress-inducible characteristic of ectopic expression of hMSH2 on RCC cells.

Both p38 MAPK and JNK Pathways Are Involved in Regulating Ectopic Expression of hMSH2 in RCC Cells in Oxidative Stress—The MAPK family plays an important role in oxidative stress-induced cellular events (28). Among the MAPK family, the activation of ERKs usually causes cell survival or differenti-

Oxidative Stress Induces Ectopic Expression of hMSH2

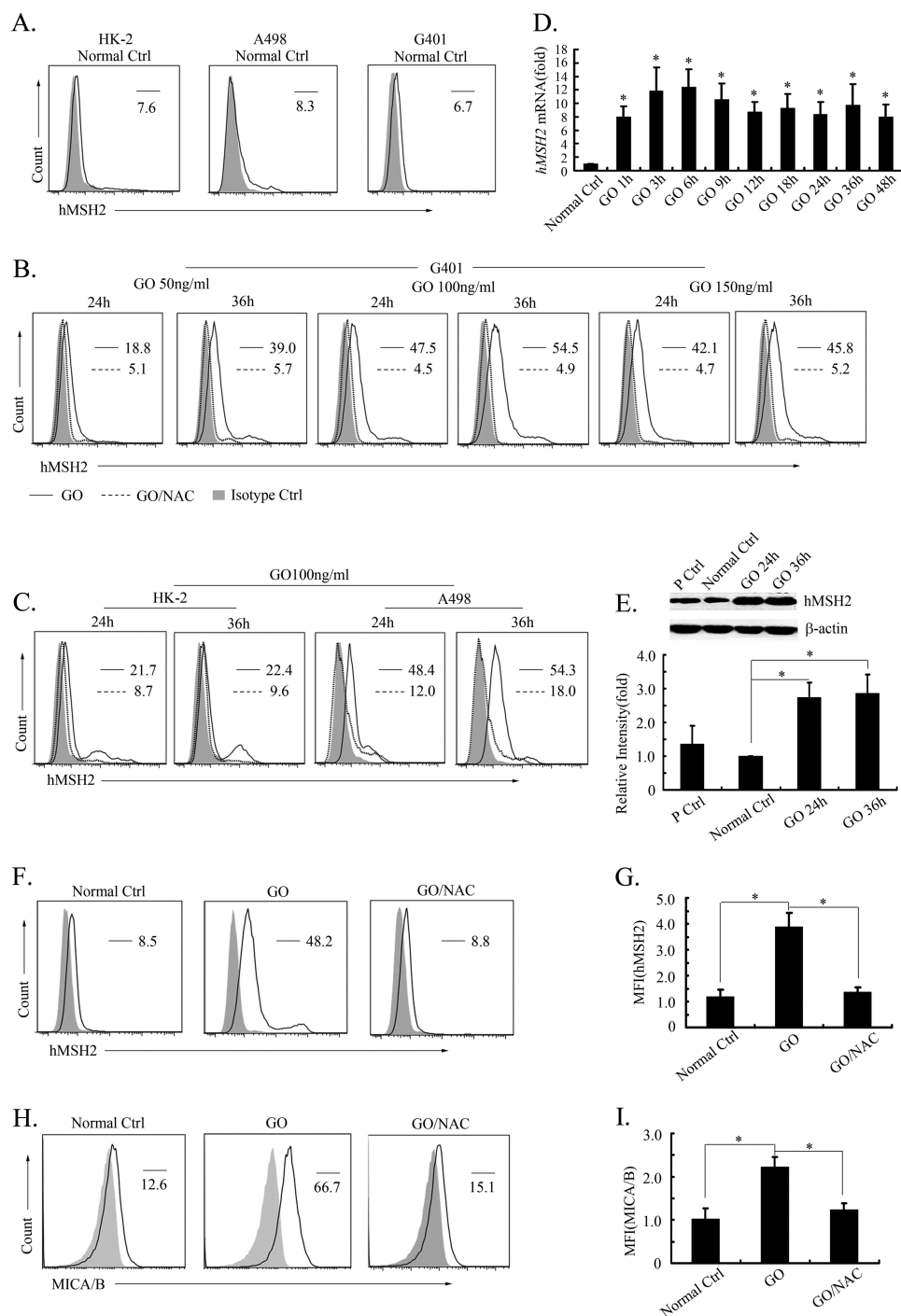


FIGURE 1. Ectopic expression of hMSH2 is inducible on human renal proximal tubule epithelial cell line HK-2 and renal carcinoma cells in oxidative stress. *A*, surface expression of hMSH2 on normal cultured HK-2 and renal carcinoma cells G401 and A498 (labeled as *Normal Ctrl*). *B* and *C*, ectopic expression of hMSH2 on the surface of HK-2, A498, and G401 cells treated with GO for 24 or 36 h. The *black lines* represent surface expression of hMSH2 on GO-stimulated cells. Surface expression of hMSH2 on GO-stimulated HK-2, A498, and G401 cells treated by NAC (5 mM) is displayed as *dotted lines*, and the respective isotype controls are shown as *solid gray*. *D*, real-time RT-PCR analysis for transcriptional expression of hMSH2 in normal or GO (100 ng/ml)-stimulated G401 cells. Data are expressed as -fold changes (mean \pm S.D. (*error bars*)) compared with the transcriptional level of hMSH2 in normal cultured G401 cells. *, $p < 0.05$. *E*, total expression of hMSH2 in whole cell extracts of normal or GO (100 ng/ml)-treated G401 cells. The total expression of hMSH2 in A375 cells is used as a positive control (*lane 1*); the total hMSH2 expression in normal control G401 cells is displayed in *lane 2*; and G401 cells GO-stimulated for 24 or 36 h, respectively, are shown in *lanes 3* and *4*. β -Actin was used as a control of protein loading (10 μ g/lane). *F-I*, comparison of ectopic expression of hMSH2 with MICA/B in oxidative stress (GO, 100 ng/ml) or adding with NAC (5 mM) into stressful cultures. Mean fluorescence intensity (MFI) values are shown as mean \pm S.D. $n = 4$ independent experiments. *, $p < 0.05$.

ation, whereas the activation of p38 MAPK and JNK pathways links to promote cell apoptosis, particularly under oxidative stress conditions (29, 30). As shown in Fig. 2, A–C, GO-induced phosphorylation of p38 MAPK (Thr-180/Tyr-182), JNK (Thr-

183/Tyr-185), and c-Jun was elevated, indicating that both p38 MAPK and JNK pathways were activated, and the MEK/ERK pathway might also present as an active state in G401 cells exposed to oxidative stress, consistent with previous studies

Oxidative Stress Induces Ectopic Expression of hMSH2

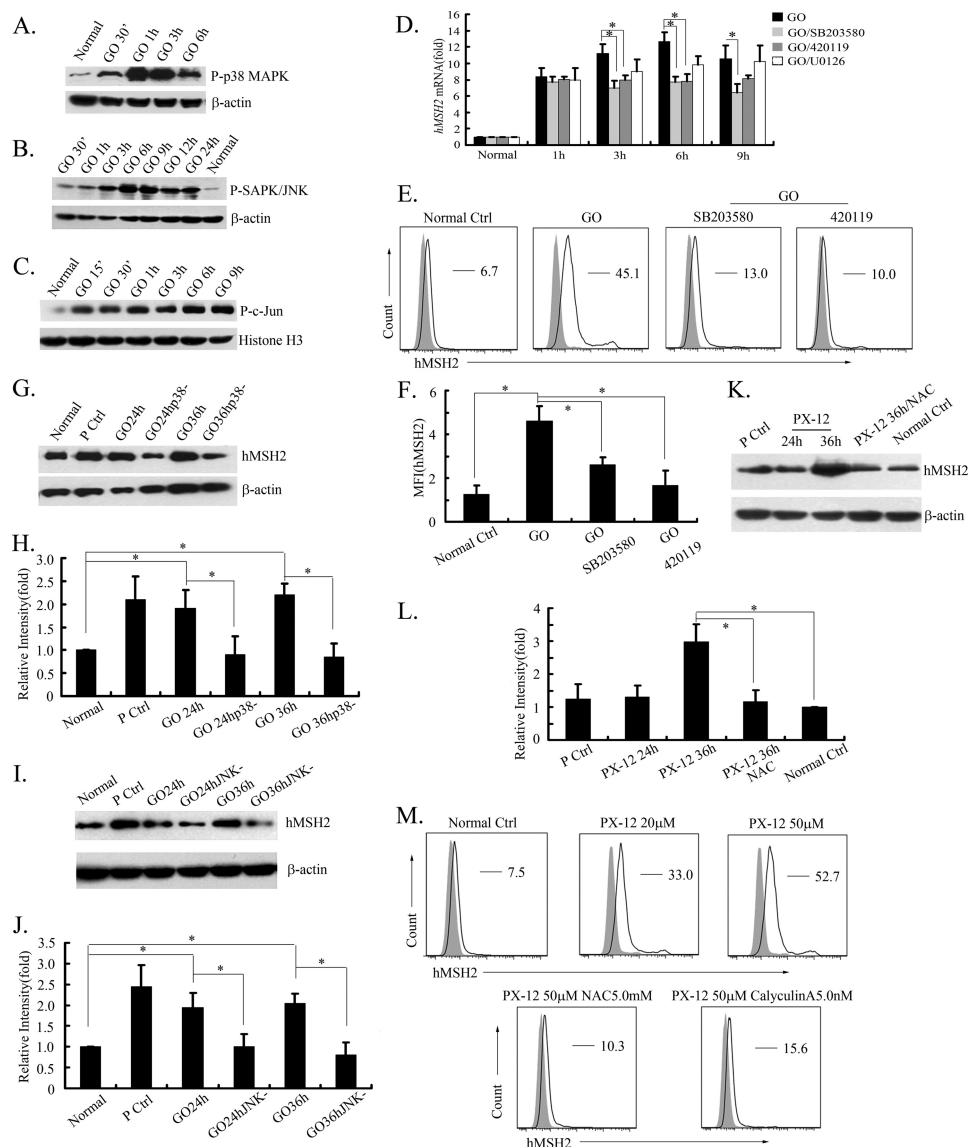


FIGURE 2. Regulatory effects of p38 MAPK and JNK pathways on ectopic expression of hMSH2 in oxidative stress. *A* and *B*, analysis of the phosphorylation (*P*-) of the p38 MAPK and JNK pathways in G401 cells at several time points after GO-mediated oxidative stress. β -Actin was used as the protein loading control (30 μ g of total proteins/lane). *C*, expression of phospho-c-Jun in G401 cells treated with GO. Histone H3 was used as the protein loading control (30 μ g of total proteins/lane). *D*, transcription of *hMSH2* in G401 cells during oxidative stress in the presence or absence of the p38 MAPK pathway inhibitor (SB203580), the JNK pathway inhibitor (420119), or the MEK/ERK pathway inhibitor (U0126) was assessed by real-time RT-PCR. Data were normalized as -fold changes (mean \pm S.D.) compared with the transcriptional level of *hMSH2* in G401 cells without GO treatment. $n = 5$ independent experiments. *, $p < 0.05$. *E* and *F*, surface expression of hMSH2 on GO (100 ng/ml)-treated G401 cells in the presence or absence of p38 MAPK or JNK pathway inhibitor ($n = 5$ independent experiments). Error bars, S.D. *, $p < 0.05$. *G–J*, total expression of hMSH2 in GO (100 ng/ml)-stimulated G401 cells treated with or without specific inhibitors for the p38 MAPK (labeled as GO p38-) or JNK (displayed as GO JNK-) pathway ($n = 4$ independent experiments). Error bars, S.D. *, $p < 0.05$. *K* and *L*, total protein expression of hMSH2 in PX-12-stimulated G401 cells. Lane 1, positive control; lanes 2 and 3, expression of hMSH2 in G401 cells treated by PX-12 (50 μ M) for 24 or 36 h, respectively (labeled as PX-12 24h and 36h). Lane 4, G401 cells treated with a combination of PX-12 (50 μ M) and NAC (5 mM). Lane 5, normal control. *M*, ectopic expression of hMSH2 on G401 cells stimulated by PX-12 in the presence or absence of NAC (5.0 mM) or calyculin A (5.0 nM) for 36 h.

(31–34). Quantitative RT-PCR detection showed that GO-induced *hMSH2* mRNA was decreased in G401 cells when pre-treated with either the specific inhibitor of p38 MAPK (SB203580) or JNK pathway (420119) (Fig. 2*D*). However, there was no significant changes of GO-induced *hMSH2* mRNA pre-treated with the MEK/ERK pathway inhibitor (Fig. 2*D*). Importantly, pretreatment with either specific inhibitor for the p38 MAPK or JNK pathway suppressed ectopic expression of hMSH2 on the surface of G401 cells induced by GO (Fig. 2, *E* and *F*), whereas inhibition of the MEK/ERK pathway showed no

obvious effects on ectopic expression of hMSH2 in oxidative stress (supplemental Fig. 1). The total expression of hMSH2 was also down-regulated when blocking the role of p38 MAPK or JNK pathway in GO-treated G401 cells (Fig. 2, *G–J*). The above data demonstrate the important roles of p38 MAPK and JNK pathways in regulating ectopic expression of hMSH2 during oxidative stress.

p38 MAPK and JNK Pathways Regulate Ectopic Expression of hMSH2 through ASK1, Node Kinase of Both Pathways—To further validate the functional involvement of the p38 MAPK and

JNK pathways in regulating ectopic expression of hMSH2 in stress, we next examined the role of ASK1, a member of the mitogen-activated protein kinase kinase kinase (MAP3K) family that could activate both JNK and p38 MAPK pathways in response to oxidative stress (35). We used the combination of PX-12 and a low level of glucose (1 g/liter) to activate ASK1 by disrupting the interaction between thioredoxin and ASK1 (36–38) and used NAC as an antioxidant to inhibit the PX-12-induced disassociation of thioredoxin from ASK1 and JNK activation (38). As shown in Fig. 2, *K–M*, both the total and ectopic expression of hMSH2 were enhanced in G401 cells when ASK1 was activated after treatment with PX-12. Meanwhile, this increase was suppressed substantially by inactivating ASK1 with NAC. To further confirm the role of activated ASK1 in enhancing ectopic expression of hMSH2, we used calyculin A, an inhibitor of protein phosphatase type 1 and 2A to inhibit the primary activation of ASK1 through inhibiting H₂O₂-induced dephosphorylation of ASK1 Ser-967 (39). It showed that PX-12-induced surface expression of hMSH2 was suppressed when dephosphorylation of ASK1 was inhibited by calyculin A (Fig. 2*M*). The effect of ASK1 on ectopic expression of hMSH2 further demonstrates the role of p38 MAPK and JNK pathways in regulating ectopic expression of hMSH2 in RCC cells.

ATF3 Acts as Executor Inducing Ectopic Expression of hMSH2 Regulated by p38 MAPK and JNK Pathways in Oxidative Stress—Activities of the activator protein 1 (AP-1) family can be stimulated by many environmental and cellular factors, including oxidative stress (40, 41). The synthesis of ATF3, a member of the AP-1 subfamily activating transcription factors, is quite robust relative to the levels of other oxidative stress-induced AP-1 proteins (42). We found that transcription factor binding sites for the AP-1 family presenting in the regulatory element of *hMSH2* were matched to ATF3 transcription factor binding sites (43–45): AP-1, –611 to –605 (5'-TGAATCA-3') and –297 to –291 (5'-TGAGTAA-3'); ATF/cAMP-response element, –1156 to –1149 (5'-TGACGTCA-3'). Therefore, we tested if ATF3 is involved in the regulation of ectopic expression of hMSH2 during oxidative stress. Interestingly, GO treatment enhanced the transcription of *ATF3* significantly at 1–3 h compared with the level in control G401 cells (Fig. 3*A*). When the GO-mediated oxidative stress was blocked by NAC, the *ATF3* transcription was down-regulated (Fig. 3*A*). Consistent with it, the total expression of ATF3 was also up-regulated in G401 cells exposed to oxidative stress (Fig. 3*B*). To investigate the potential role of ATF3 in regulating ectopic expression of hMSH2 in response to oxidative stress, *ATF3* was knocked down in G401 cells by siRNAs (Fig. 3, *C* and *D*). In response to GO-mediated oxidative stress, knocking down *ATF3* for 48 h blocked the most induction of ectopically expressed hMSH2 on G401 cells (Fig. 3, *E* and *F*). Similar *ATF3*-RNAi effects under GO-mediated oxidative stress were also observed after transfecting with *ATF3* siRNAs for 24 or 36 h (supplemental Fig. 2). However, the surface expression of MICA/B induced by oxidative stress was not affected significantly by *ATF3* knockdown (Fig. 3, *G* and *H*). Although hMSH2 and MICA/B are both stress-inducible proteins recognized by $\gamma\delta$ T cells, they show different responses of surface expression mediated by ATF3 in

stress, and ATF3 appears to play a specific role in regulating ectopic expression of hMSH2 in oxidative stress.

Proinflammatory Cytokine IL-18 Produced by RCC Cells in Oxidative Stress Is Prominent Stimulator Inducing Ectopic Expression of hMSH2—To further seek the crucial factors inducing ectopic expression or distribution of hMSH2 during oxidative stress, we noted that ROS could trigger the activation of inflammasome NLRP3/NALP3 and recruited the caspase-1 (46). The inflammasome/caspase-1 axis is essential for the maturation and release of proinflammatory cytokines, such as IL-1 β and IL-18 (46, 47). Importantly, IL-18 treatment enhances the expression of UL-16-binding protein 2 (ULBP2), a stress-inducible ligand for NKG2D in leukemia cells (48). Here, we examined whether IL-18 is a potential factor inducing ectopic expression of hMSH2 in oxidative stress. The present study showed that IL-18 was released increasingly into supernatants of GO-stimulated RCC cells (Fig. 4, *A* and *B*). IL-18 α was constitutively expressed on normal cultured G401 cells and increased in oxidative stress (Fig. 4*C*). Similar results were shown in A498 cells (data not shown). Exogenous IL-18 alone could up-regulate ectopic expression of hMSH2 in a dose-dependent manner (Fig. 4*D*). All these data indicate the potential ability of IL-18 in inducing ectopic expression of hMSH2 on RCC cells during oxidative stress. To assess the role of endogenous IL-18 in oxidative stress, siRNA-*IL-18R α* was used to knock down the expression of endogenous *IL-18R α* in G401 cells. Both levels of *IL-18R α* mRNA and protein were significantly reduced after transfection with siRNA-*IL-18R α* (Fig. 4, *E–G*). Of note, no significant up-regulation of *hMSH2* transcription or surface expression on G401 cells was found in siRNA-*IL-18R α* -treated cells (Fig. 4, *H* and *I*). The total protein level of hMSH2 in G401 cells treated with siRNA-*IL-18R α* also showed a down-regulated pattern after GO treatment (Fig. 4, *J* and *K*). These results suggest that endogenous IL-18 released by RCC cells during oxidative stress has a direct effect on inducing ectopic expression of hMSH2.

Ectopic Expression of hMSH2 Is Promoted by IFN- γ and Proinflammatory Factors Enhance Lysis of RCC Cells by $\gamma\delta$ T Cells in Oxidative Stress—Our previous studies have demonstrated that hMSH2-bearing tumor cells were susceptible to V δ 2 $\gamma\delta$ T cell-mediated cytotoxicity, in which IFN- γ and TNF- α were primary factors produced by $\gamma\delta$ T cells (15, 25, 49). It led us to examine the level of these proinflammatory cytokines produced by GO-stimulated $\gamma\delta$ T cells and their effects on ectopic expression of hMSH2. When anti-pan-TCR $\gamma\delta$ mAb-expanded $\gamma\delta$ T cells were treated with different concentrations of GO, an increased amount of IFN- γ was released into supernatants compared with $\gamma\delta$ T cells in normal cultures (Fig. 5*A*). The largest amplitude of IFN- γ in supernatant was increased from 205.78 (in normal culture) to 1027.09 pg/ml (treated with GO 50 ng/ml for 36 h), about a 5-fold increase (Fig. 5*A*). However, there was no obvious change of TNF- α upon GO treatment (Fig. 5*B*). Consistent results of the intracellular staining assay showed that the increased level of IFN- γ was mainly produced by $\gamma\delta$ T cells in GO-mediated oxidative stress (Fig. 5*C*). Then exogenous IFN- γ alone promoted GO-induced ectopic expression of hMSH2 on G401 cells, and this up-regulation was inhibited by the administration of NAC (Fig. 5, *D* and *E*). Moreover,

Oxidative Stress Induces Ectopic Expression of hMSH2

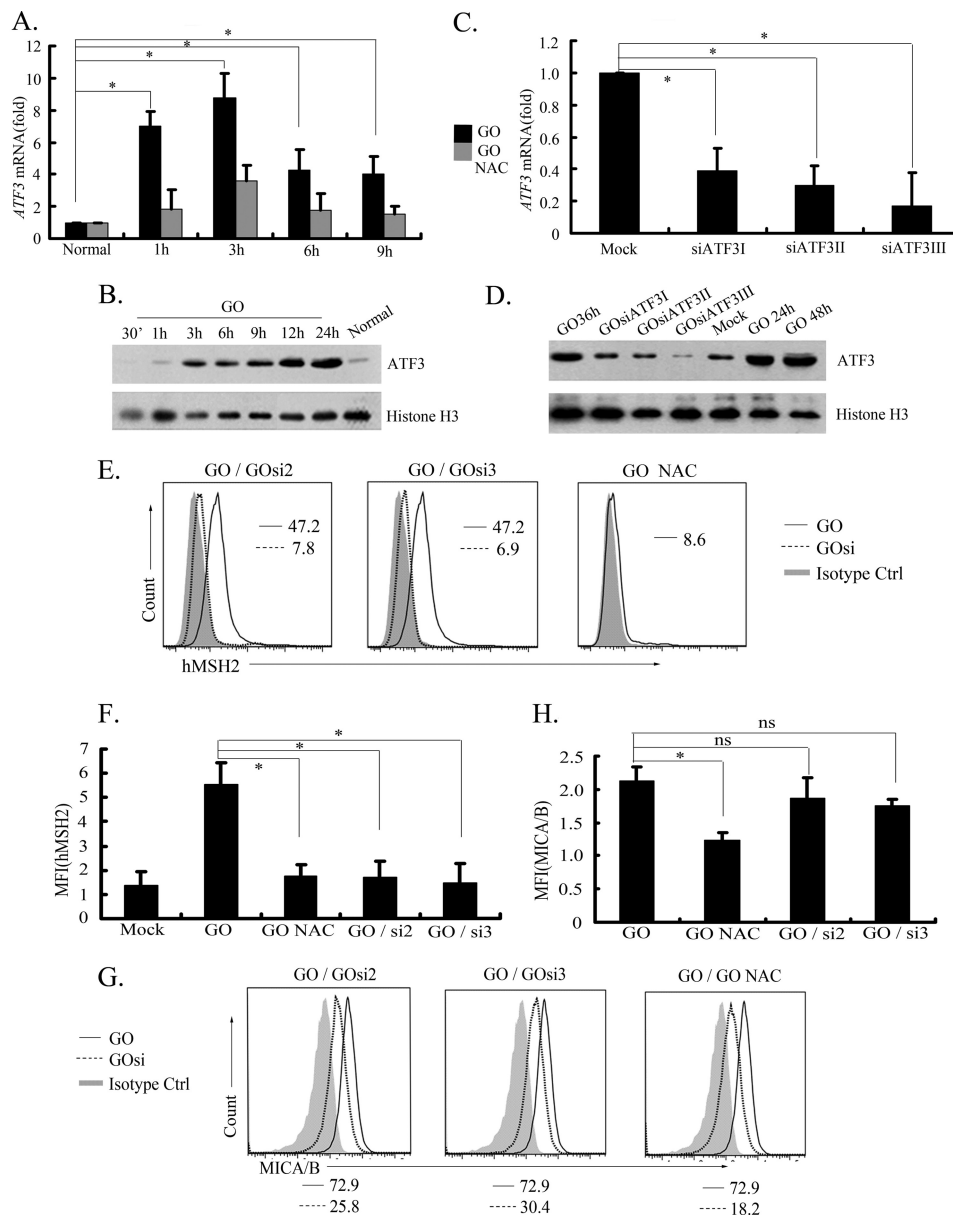


FIGURE 3. Stress-sensitive ATF3 located downstream of both p38 MAPK and JNK pathways participates in inducing ectopic expression of hMSH2 in oxidative stress. A and B, mRNA (A) and protein (B) expression of ATF3 in G401 cells at several time points after GO treatment. $n = 4$ independent experiments. Error bars, S.D. *, $p < 0.05$. Histone H3 was used as the protein loading control (30 $\mu\text{g}/\text{lane}$). C and D, mRNA and protein expression of ATF3 in G401 cells after transfection with siRNAs for ATF3. siATF3I, siATF3II, and siATF3III represented three different siRNA duplex oligoribonucleotides for ATF3. E and F, surface expression of hMSH2 on GO-stimulated G401 cells after treatment with siRNAs for ATF3. siATF3II (si2) and siATF3III (si3) were chosen for their good efficiency to knock down ATF3 expression. GO-stimulated G401 cells treated with StealthTM RNAi universal negative control duplex are depicted with *black lines*, GO-stimulated G401 cells treated with siRNAs for ATF3 (labeled as GOsi) are displayed in *dotted lines*, and the isotype controls are in *solid gray*. Mean fluorescence intensity (MF) is shown as mean \pm S.D. ($n = 3$ independent experiments). *, $p < 0.05$. G and H, MICA/B expressions on GO-stimulated G401 cells (*black line*) or ATF3-knocked down G401 cells (*dotted line*) and the isotype controls (*solid gray*). ns, no statistical significance.

the lysis of G401 cells mediated by $\gamma\delta$ T cells could be enhanced by treatment with GO, IL-18, or IL-18 plus IFN- γ (Fig. 5F). These data suggest that IFN- γ released by $\gamma\delta$ T cells in oxidative stress might promote ectopic expression of hMSH2, and the proinflammatory cytokine IL-18 or IFN- γ from oxidative stress promotes the lysis of RCC cells by $\gamma\delta$ T cells.

Ectopically Expressed hMSH2 Is Also Induced on Several Other Cancer Cell Lines in Oxidative Stress or Treatment by IL-18—To further investigate inducible ectopic expression of hMSH2 in other tumor cells, we chose the melanoma cell line A375, the lymphoma cell line Jurkat, and the leukemia cell line

K562 to analyze the surface expression of hMSH2, especially under oxidative stress or treatment with exogenous IL-18. Here, the autocrine of IL-18 in normal or stressful conditions was detected in supernatants of A375 and RCC cell lines (Fig. 6A), and all of the above tumor cells exhibited a constitutive ectopic expression of hMSH2 on their surfaces (Fig. 6B). Importantly, oxidative stress further enhanced the ectopic expression of hMSH2 on A375, Jurkat, and K562 cells (Fig. 6B). Moreover, all of these tumor cells expressed IL-18R α in normal conditions (Fig. 6C), and exogenous IL-18 could enhance ectopic expression of hMSH2 on these tumor cells (Fig. 6D).

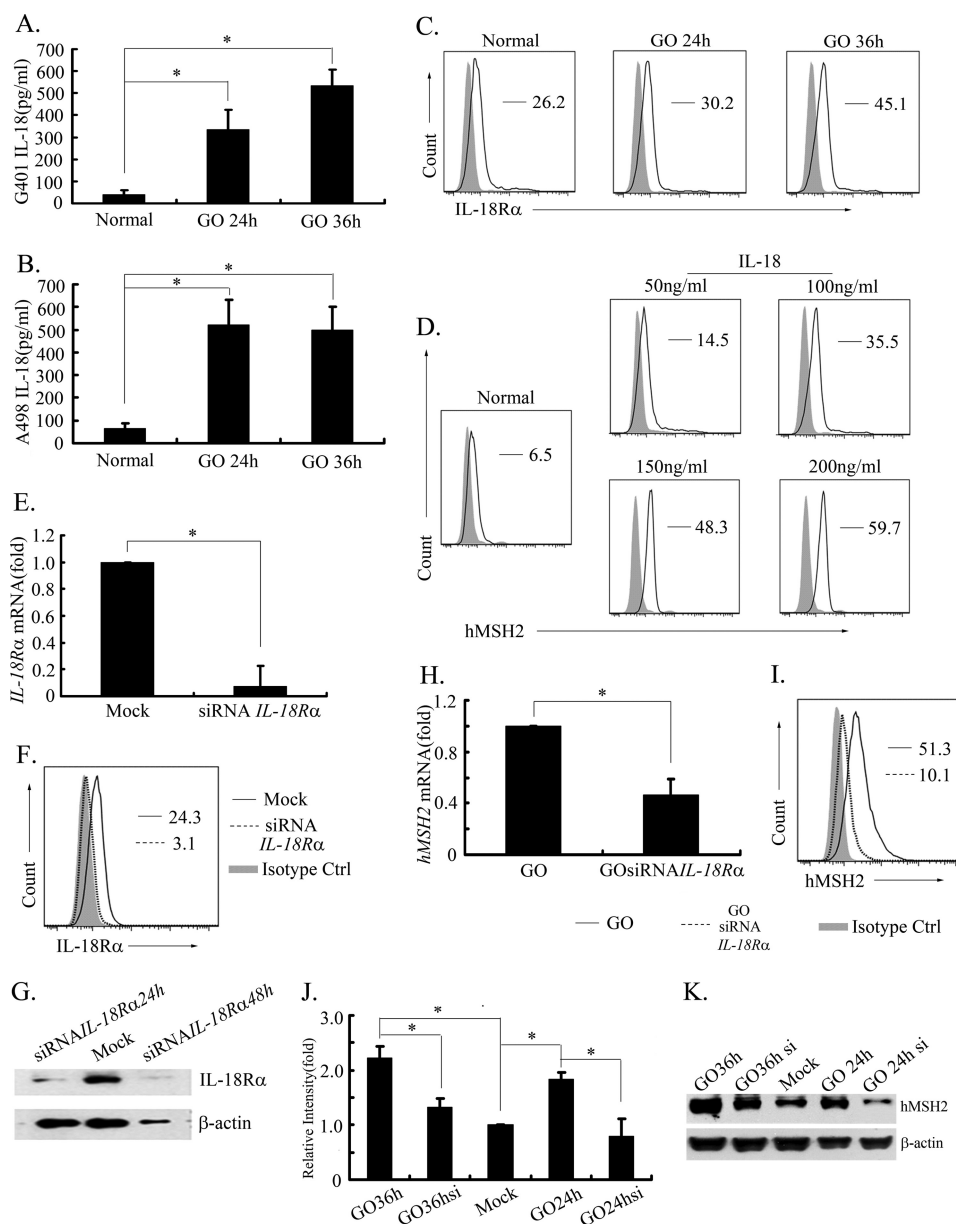


FIGURE 4. IL-18 show a direct effect on inducing ectopic expression of hMSH2 in oxidative stress. A and B, the level of IL-18 released into supernatants of G401 and A498 cells was measured by ELISA. (mean \pm S.D. (error bars); $n = 4$ independent experiments). *, $p < 0.05$. C, surface expression of IL-18R α on G401 cells (in normal culture or treated with GO (100 ng/ml) for 24 or 36 h). D, surface expression of hMSH2 on G401 cells cultured in normal conditions or treated with different doses of exogenous IL-18 for 36 h. E, normalized mRNA expression of *IL-18R α* in G401 cells after transfection with or without a pool of three-specific 19–25-nt siRNA-*IL-18R α* (mean \pm S.D.; *, $p < 0.05$). F, surface expression of IL-18R α in G401 cells on mock control siRNA-A transfected G401 cells (black line), siRNA-*IL-18R α* -transfected G401 cells (dotted line), and the isotype control (solid gray). G, expression of IL-18R α in G401 cells treated with or without a pool of three-specific siRNA-*IL-18R α* transfection. H, mRNA expression of *hMSH2* in GO-treated G401 cells after transfection with or without a pool of three-specific siRNA-*IL-18R α* (mean \pm S.D.; *, $p < 0.05$). I, surface expression of hMSH2 on GO-stimulated G401 cells after transfection with siRNA-*IL-18R α* (dotted line) or mock control siRNA-A (black line). The isotype control is labeled in solid gray. J and K, total protein expression of hMSH2 in G401 cells. GO24h or GO36h, G401 cells treated with GO for 24 or 36 h after mock control siRNA-A transfection. GO si, G401 cells treated with GO after siRNA-*IL-18R α* transfection. β -Actin was used as a control of protein loading (10 μ g of protein/lane).

These data suggest that ectopic expression of hMSH2 is broad in different tumor cells, and IL-18 induced by oxidative stress may be an important stimulator to promote ectopic hMSH2 expression on tumor cells.

DISCUSSION

Because hMSH2 participates in the removal of mispairs originating from damaged DNA in an oxidative environment (50), we have attempted to find a linkage between oxidative stress

and ectopic expression of hMSH2 on tumor cells. To mimic the stressful status in patients with several types of tumors, we chose GO-mediated oxidative stress, which is characterized by forming a continuous H_2O_2 streams into cultures at constant levels (24, 51–53). Our present findings demonstrate that expression of *hMSH2* mRNA could be enhanced in G401 cells exposed to oxidative stress. Accordingly, ectopic expression of hMSH2 is induced by GO treatment in a dose-dependent manner and blocked by a ROS scavenger, NAC. It suggests that

Oxidative Stress Induces Ectopic Expression of hMSH2

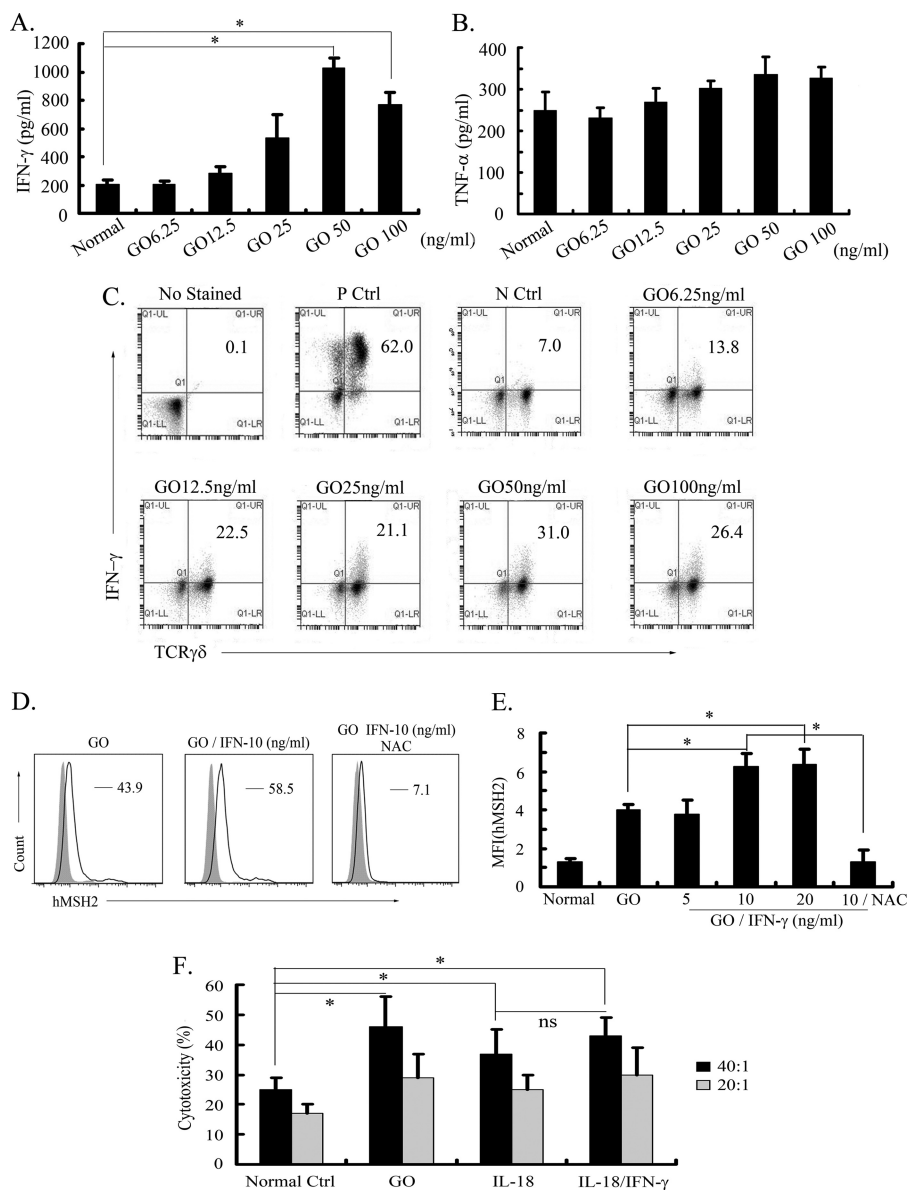


FIGURE 5. IFN- γ produced in oxidative stress promotes ectopic expression of hMSH2 and lysis of RCC cells by $\gamma\delta$ T cells. *A* and *B*, the secretion of IFN- γ or TNF- α by GO-stimulated $\gamma\delta$ T cells was measured by ELISA (mean \pm S.D.; $n = 5$ independent experiments). *, $p < 0.05$. *C*, intracellular staining detection of IFN- γ produced by GO-stimulated $\gamma\delta$ T cells. $\gamma\delta$ T cells incubated with 20 ng/ml phorbol 12-myristate-13-acetate (PMA), 0.5 μ g/ml ionomycin, and 3 μ g/ml brefeldin A for 4 h acted as the positive control. Normally cultured $\gamma\delta$ T cells incubated with 3 μ g/ml brefeldin A for 4 h are shown as the negative control. *D*, surface expression of hMSH2 on GO-stimulated G401 cells in the presence or absence of exogenous IFN- γ (10 ng/ml) followed by treatment with or without NAC (5 mM). Surface expression of hMSH2 on G401 cells is depicted with *black lines*, and the isotype controls are displayed in *solid gray*. *E*, mean fluorescence intensity (MFI) of ectopic expression of hMSH2 treated by GO with or without exogenous IFN- γ is shown. Error bar, S.D. $n = 3$ independent experiments. *, $p < 0.05$. *ns*, not significant. *F*, $\gamma\delta$ T cell-mediated lysis of G401 cells and G401 cells treated with GO (100 ng/ml), IL-18 (100 ng/ml), or IL-18 (100 ng/ml) plus IFN- γ (10 ng/ml) at E:T ratio 20:1 or 40:1. Error bars, S.D. $n = 3$ independent experiments. *, $p < 0.05$.

hMSH2 possesses the characteristic of inducible ectopic expression on the surface of RCC cells during oxidative stress. In addition, inducible ectopic expression of hMSH2 was also observed on other tumor cells, including melanoma A375, lymphoma Jurkat, and leukemia K562 cells (Fig. 6*B*). As a tumor-associated protein promoting V δ 2 $\gamma\delta$ T cell-mediated lysis (15), the inducibility of ectopically expressed hMSH2 in tumor cells indicates that it may activate many more $\gamma\delta$ T cells in certain pathological conditions, such as the oxidative stress status in patients with renal tumors, and these activated $\gamma\delta$ T cells could further recognize other ligands presenting on the surface of tumor cells and display anti-tumor cytotoxic activity. Here, the

enhanced anti-tumor immunity of $\gamma\delta$ T cells mediated by ectopic hMSH2 expression is consistent with our observation that the lysis of RCC cells by $\gamma\delta$ T cells is enhanced in oxidative stress or by proinflammatory cytokines, which could induce ectopic expression of hMSH2. Therefore, ectopically expressed hMSH2 might act as one of potential DAMPs recognized by $\gamma\delta$ T cells in stressful conditions.

Stressful states, including oxidative stress, can activate MAPK pathways (54–56). Exposure of retinal pigment epithelial cells to H₂O₂ induces apoptosis through a Rac1/JNK/p38 signaling cascade (57), and H₂O₂ also causes apoptosis by up-regulating both JNK and p38 in testicular germ cells (58). We

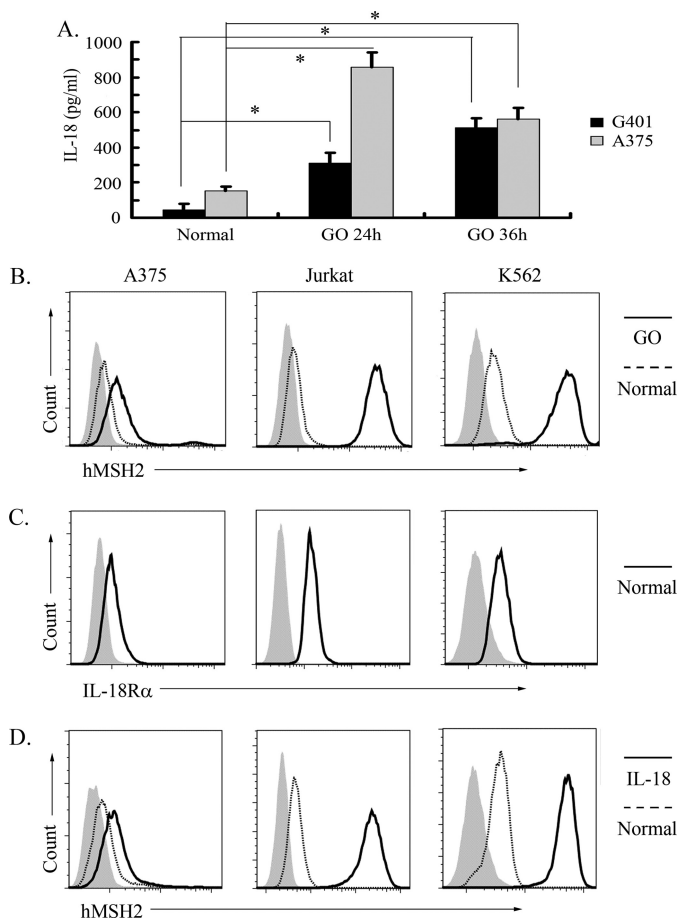


FIGURE 6. Ectopic expression of hMSH2 is inducible on human melanoma, lymphoma or leukemia cells. *A*, the level of IL-18 released into the supernatants of G401 and A375 cells was measured by ELISA (mean \pm S.D. (error bars), $n = 3$ from three independent experiments). $*$, $p < 0.05$. *B*, ectopic expression of hMSH2 on the surface of A375, Jurkat, and K562 cells stimulated with GO for 36 h. The black lines represented surface expression of hMSH2 on GO-stimulated cells. Surface expression of hMSH2 on normal cultured cells is displayed as dotted lines, and the respective isotype controls are shown as solid gray. *C*, IL-18R α expression on normal cultured A375, Jurkat, and K562 cells. *D*, ectopic expression of hMSH2 on IL-18 (100 ng/ml)-treated A375, Jurkat, and K562 cells. Shown are ectopic hMSH2 expressions on IL-18-treated tumor cells (black line), normal cultured tumor cells (dotted line), and the isotype controls (solid gray).

showed in this study that transcription factor binding sites of the AP-1 family presented in the regulatory element of *hMSH2*, and p38 MAPK and JNK pathways were activated during oxidative stress. Phosphorylated c-Jun indicated that the MEK/ERK pathway might also be active in GO-mediated oxidative stress. However, p38 MAPK and JNK but not MEK/ERK pathways indeed promoted surface expression of hMSH2 on RCC cells. The regulatory effect of p38 MAPK and JNK pathways was further confirmed by stimulating or inhibiting of ASK1, a kinase activating both MKK3/MKK6-p38 and MKK4/MKK7-JNK signaling cascades in environmental stresses (59, 60).

On the other hand, we showed that ATF3, a stress-sensitive transcription factor locating downstream of the p38 MAPK and JNK pathways (42, 61), played a crucial role in ectopic expression of hMSH2 in oxidative stress. When endogenous *ATF3* is knocked down in G401 cells, there is no significant up-regulation of ectopically expressed hMSH2 even in oxidative stress, suggesting that ATF3 may act as an executor to promote

ectopic expression of hMSH2 in an oxidative environment, although the specific mechanism needs to be clarified.

To further determine key factors regulating ectopic expression of hMSH2 on the surface of RCC cells in oxidative stress, we examined the role of IL-18, which could be produced largely by ROS-activated inflammasome NLRP3/NALP3 (46). Meanwhile, IL-18 shows the central role in promoting the inflammation and oxidative stress that lead to renal dysfunction and damage (62). Our data show that, accompanied by more IL-18 secretion, the expression of IL-18R α is up-regulated on the surface of GO-stimulated RCC cells, which leads these cells to be more sensitive to endogenous IL-18 during oxidative stress. Meanwhile, exogenous IL-18 alone effectively up-regulates surface expression of hMSH2, and GO-induced ectopic expression of hMSH2 could be inhibited by knockdown of *IL-18R α* in G401 cells. In order to identify the regulating effect of IL-18 on ectopic expression of hMSH2, we also tested the change of ectopically expressed hMSH2 on other tumor cell types, such as A375, Jurkat, and K562 cells, when treated with IL-18. Several reports have mentioned that these tumor cells could produce IL-18 under certain conditions (63–66). Interestingly, although the autocrine of IL-18 is only observed in supernatants of normal or GO-stimulated G401 and A375 cells in our study, treatment with IL-18 could induce significantly ectopic expression of hMSH2 on all of the above tumor cells. Thus, we envision that abundant IL-18 in the supernatants of stress-stimulated RCC or melanoma cells is an important stimulator inducing ectopic expression of hMSH2 on multiple types of tumor cells, including RCC, lymphoma, and leukemia. Because most hematological cancers are sensitive to the anti-tumor cytotoxicity of $\gamma\delta$ T cells (67–69) and the production of IFN- γ , GM-CSF, and TNF- α by $\gamma\delta$ T cells is strongly enhanced when treated with IL-18 (70), it suggests that IL-18 released by tumor cells in oxidative stress may promote both recognition and clearance of tumor cells by $\gamma\delta$ T cells.

We also consider proinflammatory cytokines produced by $\gamma\delta$ T cells during lysis of tumor cells (25, 49, 71, 72) and investigate their potential effects on regulating ectopic expression of hMSH2. Here, IFN- γ but not TNF- α is highly produced by GO-treated $\gamma\delta$ T cells, and exogenous IFN- γ indeed amplifies GO-induced ectopic expression of hMSH2 on G401 cells. The fact that proinflammatory cytokines IL-18 and IFN- γ in combination or alone are involved in the production of ROS in various cell types (73–76) indicates that a potential positive feedback by ROS and proinflammatory cytokines may regulate integrally ectopic expression of hMSH2 in oxidative stress. As shown in Fig. 7, oxidative stress induces ectopic expression of hMSH2 on RCC cells. Meanwhile, ROS existing in oxidative stress promote the production of IL-18 and IFN- γ by tumor cells and $\gamma\delta$ T cells, respectively. IL-18 alone could induce ectopic expression of hMSH2 on RCC cells, and both proinflammatory cytokines in turn may maintain the high level of ROS, which subsequently induces highly ectopic expression of hMSH2 presenting on the surface of RCC cells.

In conclusion, ectopically expressed hMSH2 on tumor cells possesses the inducibility in oxidative environments. The p38 MAPK and JNK pathways mainly control ectopic expression of hMSH2 on RCC cells through ASK1 upstream and stress-sen-

Oxidative Stress Induces Ectopic Expression of hMSH2

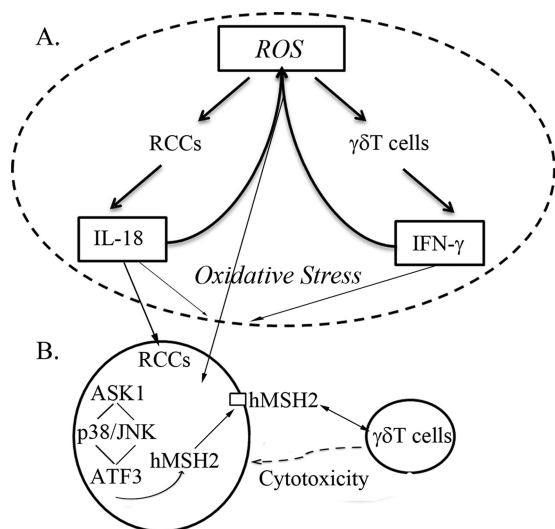


FIGURE 7. A positive feedback model for regulating ectopic expression of hMSH2 in RCC cells during oxidative stress. *A*, high level of ROS in oxidative stress causes excessive production of proinflammatory cytokines IL-18 and IFN- γ by RCC and $\gamma\delta$ T cells, respectively. IL-18 is shown as a stimulator inducing ectopic expression of hMSH2 in oxidative stress. IFN- γ promotes the above trend presenting on the surface of RCC cells. The combination of both proinflammatory cytokines in turn maintains a high level of ROS, which may further induce ectopic expression of hMSH2. *B*, in oxidative stress-stimulated RCC cells, ectopic expression of hMSH2 is controlled by p38 MAPK and JNK pathways. A node kinase ASK1 upstream and stress-sensitive ATF3 downstream of both pathways participate in the intracellular regulation of ectopic expression of hMSH2. Because hMSH2-bearing RCC cells are susceptible to $\gamma\delta$ T cell-mediated lysis, this positive feedback indicates a potential contribution of ectopically expressed hMSH2 to $\gamma\delta$ T cell-mediated immunosurveillance of tumor cells in stressful conditions.

sitive ATF3 downstream of both pathways. IL-18 produced by RCC cells is a crucial stimulator inducing ectopic expression of hMSH2 in oxidative stress, and IFN- γ produced by $\gamma\delta$ T cells might promote the above effects. Furthermore, IL-18, IFN- γ and ROS constitute a positive feedback, maintaining a high level of ectopically expressed hMSH2 on RCC cells, which promotes the lysis of RCC cells by $\gamma\delta$ T cells. All of these results suggest that inducible ectopic expression of hMSH2 on tumor cells may act as an alert signal to $\gamma\delta$ T cell-mediated immunosurveillance in stressful environments.

Acknowledgments—We thank Prof. Yuqin Liu for cell lines. Special thanks are extended to Prof. Youwen He, Dr. Jianmin Zhang, and Dr. Ning Kang for insightful comments and suggestions.

REFERENCES

- Harfe, B. D., and Jinks-Robertson, S. (2000) DNA mismatch repair and genetic instability. *Annu. Rev. Genet.* **34**, 359–399
- Li, G. M. (2008) Mechanisms and functions of DNA mismatch repair. *Cell Res.* **18**, 85–98
- Campregher, C., Luciani, M. G., and Gasche, C. (2008) Activated neutrophils induce an hMSH2-dependent G₂/M checkpoint arrest and replication errors at a (CA)₁₃-repeat in colon epithelial cells. *Gut* **57**, 780–787
- Liu, T. (2010) Mutational screening of hMLH1 and hMSH2 that confer inherited colorectal cancer susceptibility using denature gradient gel electrophoresis (DGGE). *Methods Mol. Biol.* **653**, 193–205
- Martin, S. A., Lord, C. J., and Ashworth, A. (2010) Therapeutic targeting of the DNA mismatch repair pathway. *Clin. Cancer Res.* **16**, 5107–5113
- Kastrinos, F., Stoffel, E. M., Balmaña, J., Steyerberg, E. W., Mercado, R., and Syngal, S. (2008) Phenotype comparison of MLH1 and MSH2 muta-

- tion carriers in a cohort of 1,914 individuals undergoing clinical genetic testing in the United States. *Cancer Epidemiol. Biomarkers Prev.* **17**, 2044–2051
- Altavilla, G., Fassan, M., Busatto, G., Orsolan, M., and Giacomelli, L. (2010) Microsatellite instability and hMLH1 and hMSH2 expression in renal tumors. *Oncol. Rep.* **24**, 927–932
- Acharya, S., Wilson, T., Gradia, S., Kane, M. F., Guerrette, S., Marsischky, G. T., Kolodner, R., and Fishel, R. (1996) hMSH2 forms specific mismatch-binding complexes with hMSH3 and hMSH6. *Proc. Natl. Acad. Sci. U.S.A.* **93**, 13629–13634
- Fishel, R., Lescoe, M. K., Rao, M. R., Copeland, N. G., Jenkins, N. A., Garber, J., Kane, M., and Kolodner, R. (1993) The human mutator gene homolog MSH2 and its association with hereditary nonpolyposis colon cancer. *Cell* **75**, 1027–1038
- Castrilli, G., Fabiano, A., La Torre, G., Marigo, L., Piantelli, C., Perfetti, G., Ranelletti, F. O., and Piantelli, M. (2002) Expression of hMSH2 and hMLH1 proteins of the human DNA mismatch repair system in salivary gland tumors. *J. Oral. Pathol. Med.* **31**, 234–238
- Hamid, A. A., Mandai, M., Konishi, I., Nanbu, K., Tsuruta, Y., Kusakari, T., Kariya, M., Kita, M., and Fujii, S. (2002) Cyclical change of hMSH2 protein expression in normal endometrium during the menstrual cycle and its overexpression in endometrial hyperplasia and sporadic endometrial carcinoma. *Cancer* **94**, 997–1005
- Hussein, M. R., El-Ghorori, R. M., and El-Rahman, Y. G. (2006) Alterations of p53, BCL-2, and hMSH2 protein expression in the normal brain tissues, gliosis, and gliomas. *Int. J. Exp. Pathol.* **87**, 297–306
- Hussein, M. R., Sun, M., Roggero, E., Sudilovsky, E. C., Tuthill, R. J., Wood, G. S., and Sudilovsky, O. (2002) Loss of heterozygosity, microsatellite instability, and mismatch repair protein alterations in the radial growth phase of cutaneous malignant melanomas. *Mol. Carcinog.* **34**, 35–44
- Srivastava, T., Chattopadhyay, P., Mahapatra, A. K., Sarkar, C., and Sinha, S. (2004) Increased hMSH2 protein expression in glioblastoma multiforme. *J. Neurooncol.* **66**, 51–57
- Chen, H., He, X., Wang, Z., Wu, D., Zhang, H., Xu, C., He, H., Cui, L., Ba, D., and He, W. (2008) Identification of human T cell receptor $\gamma\delta$ -recognized epitopes/proteins via CDR3 δ peptide-based immunobiochemical strategy. *J. Biol. Chem.* **283**, 12528–12537
- Ciucci, A., Gabriele, I., Percario, Z. A., Affabris, E., Colizzi, V., and Mancino, G. (2011) HMGB1 and cord blood. Its role as immunoadjuvant factor in innate immunity. *PLoS One* **6**, e23766
- Matzinger, P. (2002) The danger model. A renewed sense of self. *Science* **296**, 301–305
- Rosin, D. L., and Okusa, M. D. (2011) Dangers within. DAMP responses to damage and cell death in kidney disease. *J. Am. Soc. Nephrol.* **22**, 416–425
- Lee, S. F., and Pervaiz, S. (2011) Assessment of oxidative stress-induced DNA damage by immunofluorescent analysis of 8-oxodG. *Methods Cell Biol.* **103**, 99–113
- Frederiks, W. M., Bosch, K. S., Hoeben, K. A., van Marle, J., and Langbein, S. (2010) Renal cell carcinoma and oxidative stress. The lack of peroxisomes. *Acta Histochem.* **112**, 364–371
- Pljesa-Ercegovac, M., Mimic-Oka, J., Dragicevic, D., Savic-Radojevic, A., Opacic, M., Pljesa, S., Radosavljevic, R., and Simic, T. (2008) Altered antioxidant capacity in human renal cell carcinoma. Role of glutathione-associated enzymes. *Urol. Oncol.* **26**, 175–181
- Ahn, Y. S., Chemeris, G. Y., Turusov, V. S., and Bannasch, P. (1994) Enzymic pattern of preneoplastic and neoplastic lesions induced in the kidney of CBA mice by 1,2-dimethylhydrazine. *Toxicol. Pathol.* **22**, 415–422
- Zlatanou, A., Despras, E., Braz-Petta, T., Boubakour-Azzouz, I., Pouvelle, C., Stewart, G. S., Nakajima, S., Yasui, A., Ishchenko, A. A., and Kannonche, P. L. (2011) The hMsh2-hMsh6 complex acts in concert with monoubiquitinated PCNA and Pol η in response to oxidative DNA damage in human cells. *Mol. Cell* **43**, 649–662
- Son, Y. O., Jang, Y. S., Shi, X., and Lee, J. C. (2009) Activation of JNK and c-Jun is involved in glucose oxidase-mediated cell death of human lymphoma cells. *Mol. Cells* **28**, 545–551
- Kang, N., Zhou, J., Zhang, T., Wang, L., Lu, F., Cui, Y., Cui, L., and He, W. (2009) Adoptive immunotherapy of lung cancer with immobilized anti-TCR $\gamma\delta$ antibody-expanded human $\gamma\delta$ T-cells in peripheral blood. *Cancer*

- Biol. Ther.* **8**, 1540–1549
26. Venkataraman, G. M., Suci, D., Groh, V., Boss, J. M., and Spies, T. (2007) Promoter region architecture and transcriptional regulation of the genes for the MHC class I-related chain A and B ligands of NKG2D. *J. Immunol.* **178**, 961–969
 27. Eagle, R. A., and Trowsdale, J. (2007) Promiscuity and the single receptor. NKG2D. *Nat. Rev. Immunol.* **7**, 737–744
 28. Kyriakis, J. M., and Avruch, J. (2001) Mammalian mitogen-activated protein kinase signal transduction pathways activated by stress and inflammation. *Physiol. Rev.* **81**, 807–869
 29. Chen, L., Liu, L., and Huang, S. (2008) Cadmium activates the mitogen-activated protein kinase (MAPK) pathway via induction of reactive oxygen species and inhibition of protein phosphatases 2A and 5. *Free Radic. Biol. Med.* **45**, 1035–1044
 30. Cho, E. S., Lee, K. W., and Lee, H. J. (2008) Cocoa procyanidins protect PC12 cells from hydrogen peroxide-induced apoptosis by inhibiting activation of p38 MAPK and JNK. *Mutat. Res.* **640**, 123–130
 31. Davis, R. J. (2000) Signal transduction by the JNK group of MAP kinases. *Cell* **103**, 239–252
 32. Raugeaud, J., Gupta, S., Rogers, J. S., Dickens, M., Han, J., Ulevitch, R. J., and Davis, R. J. (1995) Proinflammatory cytokines and environmental stress cause p38 mitogen-activated protein kinase activation by dual phosphorylation on tyrosine and threonine. *J. Biol. Chem.* **270**, 7420–7426
 33. Wang, M., Atayar, C., Rosati, S., Bosga-Bouwer, A., Kluin, P., and Visser, L. (2009) JNK is constitutively active in mantle cell lymphoma. Cell cycle deregulation and polyploidy by JNK inhibitor SP600125. *J. Pathol.* **218**, 95–103
 34. Talotta, F., Mega, T., Bossis, G., Casalino, L., Basbous, J., Jariel-Encontre, I., Piechaczyk, M., and Verde, P. (2010) Heterodimerization with Fra-1 cooperates with the ERK pathway to stabilize c-Jun in response to the RAS oncoprotein. *Oncogene* **29**, 4732–4740
 35. Choi, T. G., Lee, J., Ha, J., and Kim, S. S. (2011) Apoptosis signal-regulating kinase 1 is an intracellular inducer of p38 MAPK-mediated myogenic signaling in cardiac myoblasts. *Biochem. Biophys. Acta* **1813**, 1412–1421
 36. Jordan, B. F., Runquist, M., Raghunand, N., Gillies, R. J., Tate, W. R., Powis, G., and Baker, A. F. (2005) The thioredoxin-1 inhibitor 1-methylpropyl 2-imidazolyl disulfide (PX-12) decreases vascular permeability in tumor xenografts monitored by dynamic contrast-enhanced magnetic resonance imaging. *Clin. Cancer Res.* **11**, 529–536
 37. Welsh, S. J., Williams, R. R., Birmingham, A., Newman, D. J., Kirkpatrick, D. L., and Powis, G. (2003) The thioredoxin redox inhibitors 1-methylpropyl 2-imidazolyl disulfide and pleurotin inhibit hypoxia-induced factor 1 α and vascular endothelial growth factor formation. *Mol. Cancer Ther.* **2**, 235–243
 38. Lee, Y. J., Kim, J. H., Chen, J., and Song, J. J. (2002) Enhancement of metabolic oxidative stress-induced cytotoxicity by the thioredoxin inhibitor 1-methylpropyl 2-imidazolyl disulfide is mediated through the ASK1-SEK1-JNK1 pathway. *Mol. Pharmacol.* **62**, 1409–1417
 39. Goldman, E. H., Chen, L., and Fu, H. (2004) Activation of apoptosis signal-regulating kinase 1 by reactive oxygen species through dephosphorylation at serine 967 and 14-3-3 dissociation. *J. Biol. Chem.* **279**, 10442–10449
 40. Geller, S. F., and Stone, J. (2003) Quantitative PCR analysis of FosB mRNA expression after short duration oxygen and light stress. *Adv. Exp. Med. Biol.* **533**, 249–257
 41. Hess, J., Angel, P., and Schorpp-Kistner, M. (2004) AP-1 subunits. Quarrel and harmony among siblings. *J. Cell Sci.* **117**, 5965–5973
 42. Chaum, E., Yin, J., Yang, H., Thomas, F., and Lang, J. C. (2009) Quantitative AP-1 gene regulation by oxidative stress in the human retinal pigment epithelium. *J. Cell Biochem.* **108**, 1280–1291
 43. Filén, S., Ylikoski, E., Tripathi, S., West, A., Bjorkman, M., Nystrom, J., Ahlfors, H., Coffey, E., Rao, K. V., Rasool, O., and Lahesmaa, R. (2010) Activating transcription factor 3 is a positive regulator of human IFNG gene expression. *J. Immunol.* **184**, 4990–4999
 44. St Germain, C., Niknejad, N., Ma, L., Garbuio, K., Hai, T., and Dimitroulakos, J. (2010) Cisplatin induces cytotoxicity through the mitogen-activated protein kinase pathways and activating transcription factor 3. *Neoplasia* **12**, 527–538
 45. Scherer, S. J., Maier, S. M., Seifert, M., Hanselmann, R. G., Zang, K. D., Muller-Hermelink, H. K., Angel, P., Welter, C., and Schartl, M. (2000) p53 and c-Jun functionally synergize in the regulation of the DNA repair gene hMSH2 in response to UV. *J. Biol. Chem.* **275**, 37469–37473
 46. Martinon, F. (2010) Signaling by ROS drives inflammasome activation. *Eur. J. Immunol.* **40**, 616–619
 47. Dostert, C., Pétrilli, V., Van Bruggen, R., Steele, C., Mossman, B. T., and Tschopp, J. (2008) Innate immune activation through Nalp3 inflammasome sensing of asbestos and silica. *Science* **320**, 674–677
 48. Song, H., Kim, K. E., Hur, D., Lim, J. S., Yang, Y., Cho, B. J., Kim, C. H., Kim, T., Bang, S., Lee, W. J., Park, H., and Cho, D. (2008) IL-18 enhances ULBP2 expression through the MAPK pathway in leukemia cells. *Immunol. Lett.* **120**, 103–107
 49. Gao, Y., Yang, W., Pan, M., Scully, E., Girardi, M., Augenlicht, L. H., Craft, J., and Yin, Z. (2003) $\gamma\delta$ T cells provide an early source of interferon γ in tumor immunity. *J. Exp. Med.* **198**, 433–442
 50. Martin, S. A., McCarthy, A., Barber, L. J., Burgess, D. J., Parry, S., Lord, C. J., and Ashworth, A. (2009) Methotrexate induces oxidative DNA damage and is selectively lethal to tumor cells with defects in the DNA mismatch repair gene *MSH2*. *EMBO Mol. Med.* **1**, 323–337
 51. Son, Y. O., Jang, Y. S., Heo, J. S., Chung, W. T., Choi, K. C., and Lee, J. C. (2009) Apoptosis-inducing factor plays a critical role in caspase-independent, pyknotic cell death in hydrogen peroxide-exposed cells. *Apoptosis* **14**, 796–808
 52. Maddux, B. A., See, W., Lawrence, J. C., Jr., Goldfine, A. L., Goldfine, I. D., and Evans, J. L. (2001) Protection against oxidative stress-induced insulin resistance in rat L6 muscle cells by micromolar concentrations of α -lipoic acid. *Diabetes* **50**, 404–410
 53. Rudich, A., Tirosh, A., Potashnik, R., Hemi, R., Kanety, H., and Bashan, N. (1998) Prolonged oxidative stress impairs insulin-induced GLUT4 translocation in 3T3-L1 adipocytes. *Diabetes* **47**, 1562–1569
 54. Lee, J. C., Laydon, J. T., McDonnell, P. C., Gallagher, T. F., Kumar, S., Green, D., McNulty, D., Blumenthal, M. J., Heys, J. R., and Landvatter, S. W. (1994) A protein kinase involved in the regulation of inflammatory cytokine biosynthesis. *Nature* **372**, 739–746
 55. Maroney, A. C., Glicksman, M. A., Basma, A. N., Walton, K. M., Knight, E., Jr., Murphy, C. A., Bartlett, B. A., Finn, J. P., Angeles, T., Matsuda, Y., Neff, N. T., and Dionne, C. A. (1998) Motoneuron apoptosis is blocked by CEP-1347 (KT 7515), a novel inhibitor of the JNK signaling pathway. *J. Neurosci.* **18**, 104–111
 56. Nijhawan, D., Honarpour, N., and Wang, X. (2000) Apoptosis in neural development and disease. *Annu. Rev. Neurosci.* **23**, 73–87
 57. Ho, T. C., Yang, Y. C., Cheng, H. C., Wu, A. C., Chen, S. L., Chen, H. K., and Tsao, Y. P. (2006) Activation of mitogen-activated protein kinases is essential for hydrogen peroxide-induced apoptosis in retinal pigment epithelial cells. *Apoptosis* **11**, 1899–1908
 58. Maheshwari, A., Misro, M. M., Aggarwal, A., Sharma, R. K., and Nandan, D. (2009) Pathways involved in testicular germ cell apoptosis induced by H₂O₂ *in vitro*. *FEBS J.* **276**, 870–881
 59. Ichijo, H. (1999) From receptors to stress-activated MAP kinases. *Oncogene* **18**, 6087–6093
 60. Ichijo, H., Nishida, E., Irie, K., ten Dijke, P., Saitoh, M., Moriguchi, T., Takagi, M., Matsumoto, K., Miyazono, K., and Gotoh, Y. (1997) Induction of apoptosis by ASK1, a mammalian MAPKKK that activates SAPK/JNK and p38 signaling pathways. *Science* **275**, 90–94
 61. Miyazaki, K., Inoue, S., Yamada, K., Watanabe, M., Liu, Q., Watanabe, T., Adachi, M. T., Tanaka, Y., and Kitajima, S. (2009) Differential usage of alternate promoters of the human stress response gene ATF3 in stress response and cancer cells. *Nucleic Acids Res.* **37**, 1438–1451
 62. Khanna, A. (2011) Interleukin-18, a potential mediator of inflammation, oxidative stress, and allograft dysfunction. *Transplantation* **91**, 590–591
 63. Bachmann, M., Dragoi, C., Poleganov, M. A., Pfeilschifter, J., and Mühl, H. (2007) Interleukin-18 directly activates T-bet expression and function via p38 mitogen-activated protein kinase and nuclear factor- κ B in acute myeloid leukemia-derived predendritic KG-1 cells. *Mol. Cancer Ther.* **6**, 723–731
 64. Kiersnowska-Rogowska, B., Izycka, A., Jabłońska, E., Rogowski, F., and Parfieniecyk, A. (2005) [Estimation of level of soluble form PECAM-1, ICAM-2, TNF- α , and IL-18 in serum patients with chronic myelogenic

Oxidative Stress Induces Ectopic Expression of hMSH2

- leukemia]. *Przegląd lekarski*. **62**, 772–774
65. Ogata, A., Kitano, M., Fukamizu, M., Hamano, T., and Sano, H. (2004) Increased serum interleukin-18 in a patient with systemic lupus erythematosus and T-cell large granular lymphocytic leukemia. *Mod. Rheumatol.* **14**, 267–270
66. Park, S., Kim, T. S., Kim, C., Kim, S., Bang, S. I., Park, H., and Cho, D. H. (2009) Transferrin induces interleukin-18 expression in chronic myeloid leukemia cell line, K-562. *Leuk. Res.* **33**, 315–320
67. Saitoh, A., Narita, M., Watanabe, N., Tochiki, N., Satoh, N., Takizawa, J., Furukawa, T., Toba, K., Aizawa, Y., Shinada, S., and Takahashi, M. (2008) Anti-tumor cytotoxicity of $\gamma\delta$ T cells expanded from peripheral blood cells of patients with myeloma and lymphoma. *Med. Oncol.* **25**, 137–147
68. Kunzmann, V., and Wilhelm, M. (2005) Anti-lymphoma effect of $\gamma\delta$ T cells. *Leukemia Lymphoma* **46**, 671–680
69. Wilhelm, M., Kunzmann, V., Eckstein, S., Reimer, P., Weissinger, F., Ruediger, T., and Tony, H. P. (2003) $\gamma\delta$ T cells for immune therapy of patients with lymphoid malignancies. *Blood* **102**, 200–206
70. Li, W., Kubo, S., Okuda, A., Yamamoto, H., Ueda, H., Tanaka, T., Nakamura, H., Yamanishi, H., Terada, N., and Okamura, H. (2010) Effect of IL-18 on expansion of $\gamma\delta$ T cells stimulated by zoledronate and IL-2. *J. Immunother.* **33**, 287–296
71. Todaro, M., D'Asaro, M., Caccamo, N., Iovino, F., Francipane, M. G., Meraviglia, S., Orlando, V., La Mendola, C., Gulotta, G., Salerno, A., Dieli, F., and Stassi, G. (2009) Efficient killing of human colon cancer stem cells by $\gamma\delta$ T lymphocytes. *J. Immunol.* **182**, 7287–7296
72. Kondo, M., Sakuta, K., Noguchi, A., Ariyoshi, N., Sato, K., Sato, S., Sato, K., Hosoi, A., Nakajima, J., Yoshida, Y., Shiraishi, K., Nakagawa, K., and Kakimi, K. (2008) Zoledronate facilitates large-scale *ex vivo* expansion of functional $\gamma\delta$ T cells from cancer patients for use in adoptive immunotherapy. *Cytotherapy* **10**, 842–856
73. Qi, X. F., Teng, Y. C., Yoon, Y. S., Kim, D. H., Cai, D. Q., and Lee, K. J. (2011) Reactive oxygen species are involved in the IFN- γ -stimulated production of Th2 chemokines in HaCaT keratinocytes. *J. Cell Physiol.* **226**, 58–65
74. Venkatesan, B., Valente, A. J., Reddy, V. S., Siwik, D. A., and Chandrasekar, B. (2009) Resveratrol blocks interleukin-18-EMMPRIN cross-regulation and smooth muscle cell migration. *Am. J. Physiol. Heart Circ. Physiol.* **297**, H874–H886
75. Wyman, T. H., Dinarello, C. A., Banerjee, A., Gamboni-Robertson, F., Hiester, A. A., England, K. M., Kelher, M., and Silliman, C. C. (2002) Physiological levels of interleukin-18 stimulate multiple neutrophil functions through p38 MAP kinase activation. *J. Leukocyte Biol.* **72**, 401–409
76. Yang, D., Elner, S. G., Bian, Z. M., Till, G. O., Petty, H. R., and Elner, V. M. (2007) Pro-inflammatory cytokines increase reactive oxygen species through mitochondria and NADPH oxidase in cultured RPE cells. *Exp. Eye Res.* **85**, 462–472
77. Dai, Y., Chen, H., Mo, C., Cui, L., and He, W. (March 20, 2012) Ectopically expressed human tumor biomarker MutS homologue 2 is a novel endogenous ligand that is recognized by human $\gamma\delta$ T cells to induce innate anti-tumor/virus immunity. *J. Biol. Chem.* **287**, 10.1074/jbc.M111.327650